

$B \rightarrow \pi\rho, \pi\omega$ Decays in Perturbative QCD Approach

Cai-Dian Lü, Mao-Zhi Yang

CCAST (World Laboratory), P.O. Box 8730, Beijing 100080, China;

Institute of High Energy Physics, CAS, P.O. Box 918(4), Beijing 100039, China*

and

Physics Department, Hiroshima University, Higashi-Hiroshima 739-8526, Japan

April 26, 2024

Abstract

We calculate the branching ratios and CP asymmetries for $B^0 \rightarrow \pi^+\rho^-$, $B^0 \rightarrow \rho^+\pi^-$, $B^+ \rightarrow \rho^+\pi^0$, $B^+ \rightarrow \pi^+\rho^0$, $B^0 \rightarrow \pi^0\rho^0$, $B^+ \rightarrow \pi^+\omega$ and $B^0 \rightarrow \pi^0\omega$ decays, in a perturbative QCD approach. In this approach, we calculate non-factorizable and annihilation type contributions, in addition to the usual factorizable contributions. Our result is in agreement with the measured branching ratio of $B^0/\bar{B}^0 \rightarrow \pi^\pm\rho^\mp$, $B^\pm \rightarrow \pi^\pm\rho^0$, $\pi^\pm\omega$ by CLEO and BABAR collaboration. We also predict large CP asymmetries in these decays. These channels are useful to determine the CKM angle ϕ_2 .

PACS: 13.25.Hw, 11.10.Hi, 12.38.Bx,

*Mailing address

1 Introduction

The rare decays of B mesons are getting more and more interesting, since they are useful for search of CP violation and sensitive to new physics. The recent measurement of $B \rightarrow \pi\rho$ and $\pi\omega$ decays by CLEO Collaboration [1] arouse more discussions on these decays [2]. The $B \rightarrow \pi\rho$, $\pi\omega$ decays which are helpful to the determination of Cabbibo-Kobayashi-Maskawa (CKM) unitarity triangle ϕ_2 have been studied in the factorization approach in detail [3, 4]. In this paper, we would like to study the $B \rightarrow \pi\rho$ and $\pi\omega$ decays in the perturbative QCD approach (PQCD), where we can calculate the non-factorizable contributions as corrections to the usual factorization approach.

In the $B \rightarrow \pi\rho$, $\pi\omega$ decays, the B meson is heavy, sitting at rest. It decays into two light mesons with large momenta. Therefore the light mesons are moving very fast in the rest frame of B meson. In this case, the short distance hard process dominates the decay amplitude. The reasons can be ordered as: first, because there are not many resonances near the energy region of B mass, so it is reasonable to assume that final state interaction is not important in two-body B decays. Second, With the final light mesons moving very fast, there must be a hard gluon to kick the light spectator quark (almost at rest) in the B meson to form a fast moving pion or light vector meson. So the dominant diagram in this theoretical picture is that one hard gluon from the spectator quark connecting with the other quarks in the four quark operator of the weak interaction. There are also soft (soft and collinear) gluon exchanges between quarks. Summing over those leading soft contributions gives a Sudakov form factor, which suppresses the soft contribution to be dominant. Therefore, it makes the PQCD reliable in calculating the non-leptonic decays. With the Sudakov resummation, we can include the leading double logarithms for all loop diagrams, in association with the soft contribution. Unlike the usual factorization approach, the hard part of the PQCD approach consists of six quarks rather than four. We thus call it six-quark operators or six-quark effective theory. Applying the six-quark effective theory to B meson decays, we need meson wave functions for the hadronization of quarks into mesons. All the collinear dynamics are included in the meson wave functions.

In this paper, we calculate the $B \rightarrow \pi$ and $B \rightarrow \rho$ form factors, which are input parameters used in factorization approach. The form factor calculations can give severe restrictions to the input meson wave functions. We also calculate the non-factorizable contributions and the

annihilation type diagrams, which are difficult to calculate in the factorization approach. We found that this type of diagrams give dominant contributions to strong phases. The strong phase in this approach can also be calculated directly, without ambiguity. In the next section, we will briefly introduce our method of PQCD. In section 3, we perform the perturbative calculations for all the channels. And we give the numerical results and discussions in section 4. Finally section 5 is a short summary.

2 The Frame Work

The three scale PQCD factorization theorem has been developed for non-leptonic heavy meson decays [5]. The factorization formula is given by the typical expression,

$$C(t) \times H(x, t) \times \Phi(x) \times \exp \left[-s(P, b) - 2 \int_{1/b}^t \frac{d\bar{\mu}}{\bar{\mu}} \gamma_q(\alpha_s(\bar{\mu})) \right], \quad (1)$$

where $C(t)$ are the corresponding Wilson coefficients, $\Phi(x)$ are the meson wave functions. And the quark anomalous dimension $\gamma_q = -\alpha_s/\pi$ describes the evolution from scale t to $1/b$.

Non-leptonic heavy meson decays involve three scales: the W boson mass m_W , at which the matching condition of the effective Hamiltonian are defined, the typical scale t of a hard subamplitude, which reflects the dynamics of heavy quark decays, and the factorization scale $1/b$, with b the conjugate variable of parton transverse momenta. The dynamics below $1/b$ scale is regarded as being completely non-perturbative, and can be parameterized into meson wave functions. Above the scale $1/b$, PQCD is reliable and radiative corrections produce two types of large logarithms: $\ln(m_W/t)$ and $\ln(tb)$. The former are summed by renormalization group equations to give the leading logarithm evolution from m_W to t scale contained in the Wilson coefficients $C(t)$. While the latter are summed to give the evolution from t scale down to $1/b$, shown as the last factor in eq.(1).

There exist also double logarithms $\ln^2(Pb)$ from the overlap of collinear and soft divergence, P being the dominant light-cone component of a meson momentum. The resummation of these double logarithms leads to a Sudakov form factor $\exp[-s(P, b)]$, which suppresses the long distance contributions in the large b region, and vanishes as $b > 1/\Lambda_{QCD}$. This factor improves the applicability of PQCD. For the detailed derivation of the Sudakov form factors,

see ref.[6, 7]. Since all logarithm corrections have been summed by renormalization group equations, the above factorization formula does not depend on the renormalization scale μ .

With all the large logarithms resummed, the remaining finite contributions are absorbed into a hard sub-amplitude $H(x, t)$. The $H(x, t)$ are calculated perturbatively involving the four quark operators together with the spectator quark, connected by a hard gluon. When the end-point region ($x \rightarrow 0, 1$) of wave function is important for the hard amplitude, the corresponding large double logarithms $\alpha_s \ln^2 x$ shall appear in the hard amplitude $H(x, t)$, which should be resummed to give a jet function $S_t(x)$. This technique is the so-called threshold resummation [8]. The threshold resummation form factor $S_t(x)$ vanishes as $x \rightarrow 0, 1$, which effectively suppresses the end-point behavior of the hard amplitude. This suppression will become important when the meson wave function remains constant at the end-point region. For example, the twist-3 wave function ϕ_π^P and ϕ_π^t are such kinds of wave functions, which can be found in the numerical section of this paper. The typical scale t in the hard sub-amplitude is around $\sqrt{\Lambda M_B}$. It is chosen as the maximum value of those scales appeared in the six quark action. This is to diminish the α_s^2 corrections to the six quark amplitude. The expression of scale t in different sub-amplitude will be derived in the next section and the formula is showed in the appendix.

2.1 Wilson Coefficients

First we begin with the weak effective Hamiltonian H_{eff} for the $\Delta B = 1$ transitions as

$$\mathcal{H}_{eff} = \frac{G_F}{\sqrt{2}} \left[V_{ub}V_{ud}^* (C_1 O_1^u + C_2 O_2^u) - V_{tb}V_{td}^* \sum_{i=3}^{10} C_i O_i \right] . \quad (2)$$

We specify below the operators in \mathcal{H}_{eff} for $b \rightarrow d$:

$$\begin{aligned} O_1^u &= \bar{d}_\alpha \gamma^\mu L u_\beta \cdot \bar{u}_\beta \gamma_\mu L b_\alpha , & O_2^u &= \bar{d}_\alpha \gamma^\mu L u_\alpha \cdot \bar{u}_\beta \gamma_\mu L b_\beta , \\ O_3 &= \bar{d}_\alpha \gamma^\mu L b_\alpha \cdot \sum_{q'} \bar{q}'_\beta \gamma_\mu L q'_\beta , & O_4 &= \bar{d}_\alpha \gamma^\mu L b_\beta \cdot \sum_{q'} \bar{q}'_\beta \gamma_\mu L q'_\alpha , \\ O_5 &= \bar{d}_\alpha \gamma^\mu L b_\alpha \cdot \sum_{q'} \bar{q}'_\beta \gamma_\mu R q'_\beta , & O_6 &= \bar{d}_\alpha \gamma^\mu L b_\beta \cdot \sum_{q'} \bar{q}'_\beta \gamma_\mu R q'_\alpha , \\ O_7 &= \frac{3}{2} \bar{d}_\alpha \gamma^\mu L b_\alpha \cdot \sum_{q'} e_{q'} \bar{q}'_\beta \gamma_\mu R q'_\beta , & O_8 &= \frac{3}{2} \bar{d}_\alpha \gamma^\mu L b_\beta \cdot \sum_{q'} e_{q'} \bar{q}'_\beta \gamma_\mu R q'_\alpha , \\ O_9 &= \frac{3}{2} \bar{d}_\alpha \gamma^\mu L b_\alpha \cdot \sum_{q'} e_{q'} \bar{q}'_\beta \gamma_\mu L q'_\beta , & O_{10} &= \frac{3}{2} \bar{d}_\alpha \gamma^\mu L b_\beta \cdot \sum_{q'} e_{q'} \bar{q}'_\beta \gamma_\mu L q'_\alpha . \end{aligned} \quad (3)$$

Here α and β are the $SU(3)$ color indices; L and R are the left- and right-handed projection operators with $L = (1 - \gamma_5)$, $R = (1 + \gamma_5)$. The sum over q' runs over the quark fields that are active at the scale $\mu = O(m_b)$, i.e., $(q' \in \{u, d, s, c, b\})$.

The PQCD approach works well for the leading twist approximation and leading double logarithm summation. For the Wilson coefficients, we will also use the leading logarithm summation for the QCD corrections, although the next-to-leading order calculations already exist in the literature [9]. This is the consistent way to cancel the explicit μ dependence in the theoretical formulae.

If the scale $m_b < t < m_W$, then we evaluate the Wilson coefficients at t scale using leading logarithm running equations [9], in the appendix B of ref.[10]. In numerical calculations, we use $\alpha_s = 4\pi/[\beta_1 \ln(t^2/\Lambda_{QCD}^{(5)})^2]$ which is the leading order expression with $\Lambda_{QCD}^{(5)} = 193\text{MeV}$, derived from $\Lambda_{QCD}^{(4)} = 250\text{MeV}$. Here $\beta_1 = (33 - 2n_f)/12$, with the appropriate number of active quarks n_f . $n_f = 5$ when scale t is larger than m_b .

If the scale $t < m_b$, then we evaluate the Wilson coefficients at t scale using the formulae in appendix C of ref.[10] for four active quarks ($n_f = 4$) (again in leading logarithm approximation).

2.2 Wave Functions

In the resummation procedures, the B meson is treated as a heavy-light system. In general, the B meson light-cone matrix element can be decomposed as [11, 12]

$$\begin{aligned} & \int_0^1 \frac{d^4 z}{(2\pi)^4} e^{i\mathbf{k}_1 \cdot \mathbf{z}} \langle 0 | \bar{b}_\alpha(0) d_\beta(z) | B(p_B) \rangle \\ &= -\frac{i}{\sqrt{2N_c}} \left\{ (\not{n}_B + m_B) \gamma_5 \left[\phi_B(\mathbf{k}_1) - \frac{\not{n}_- \not{n}_+}{\sqrt{2}} \bar{\phi}_B(\mathbf{k}_1) \right] \right\}_{\beta\alpha}, \end{aligned} \quad (4)$$

where $n = (1, 0, \mathbf{0}_T)$, and $v = (0, 1, \mathbf{0}_T)$ are the unit vectors pointing to the plus and minus directions, respectively. From the above equation, one can see that there are two Lorentz structures in the B meson distribution amplitudes. They obey to the following normalization conditions

$$\int \frac{d^4 k_1}{(2\pi)^4} \phi_B(\mathbf{k}_1) = \frac{f_B}{2\sqrt{2N_c}}, \quad \int \frac{d^4 k_1}{(2\pi)^4} \bar{\phi}_B(\mathbf{k}_1) = 0. \quad (5)$$

In general, one should consider both these two Lorentz structures in calculations of B meson decays. However, it can be argued that the contribution of $\bar{\phi}_B$ is numerically small [13], thus its contribution can be numerically neglected. Therefore, we only consider the contribution of

Lorentz structure

$$\Phi_B = \frac{1}{\sqrt{2N_c}}(\not{p}_B + m_B)\gamma_5\phi_B(\mathbf{k}_1), \quad (6)$$

in our calculation. We keep the same input as other calculations in this direction [10, 13, 14] and it is also easier for comparing with other approaches [12, 15]. Through out this paper, we use the light-cone coordinates to write the four momentum as $(k_1^+, k_1^-, k_1^\perp)$. In the next section, we will see that the hard part is always independent of one of the k_1^+ and/or k_1^- , if we make some approximations. The B meson wave function is then the function of variable k_1^- (or k_1^+) and k_1^\perp .

$$\phi_B(k_1^-, k_1^\perp) = \int dk_1^+ \phi(k_1^+, k_1^-, k_1^\perp). \quad (7)$$

The π meson is treated as a light-light system. At the B meson rest frame, pion is moving very fast, one of k_1^+ or k_1^- is zero depends on the definition of the z axis. We consider a pion moving in the minus direction in this paper. The pion distribution amplitude is defined by [16]

$$\begin{aligned} & \langle \pi^-(P) | \bar{d}_\alpha(z) u_\beta(0) | 0 \rangle \\ &= \frac{i}{\sqrt{2N_c}} \int_0^1 e^{ixP \cdot z} \left[\gamma_5 \not{P} \phi_\pi(x) + m_0 \gamma_5 \phi_P(x) - m_0 \sigma^{\mu\nu} \gamma_5 P_\mu z_\nu \frac{\phi_\sigma(x)}{6} \right]_{\beta\alpha} \end{aligned} \quad (8)$$

For the first and second terms in the above equation, we can easily get the projector of the distribution amplitude in the momentum space. However, for the third term we should make some effort to transfer it into the momentum space. By using integration by parts for the third term, after a few steps, eq.(8) can be finally changed to be

$$\begin{aligned} & \langle \pi^-(P) | \bar{d}_\alpha(z) u_\beta(0) | 0 \rangle \\ &= \frac{i}{\sqrt{2N_c}} \int_0^1 e^{ixP \cdot z} \left[\gamma_5 \not{P} \phi_\pi(x) + m_0 \gamma_5 \phi_P(x) + m_0 [\gamma_5 (\not{v} \not{v} - 1)] \phi_\pi^t(x) \right]_{\beta\alpha} \end{aligned} \quad (9)$$

where $\phi_\pi^t(x) = \frac{1}{6} \frac{d}{dx} \phi_\sigma(x)$, and vector v is parallel to the π meson momentum p_π . And $m_0 = m_\pi^2/(m_u + m_d)$ is a scale characterized by the Chiral perturbation theory. In $B \rightarrow \pi\rho$ decays, ρ meson is only longitudinally polarized. We only consider its wave function in longitudinal polarization [13, 17].

$$\langle \rho^-(P, \epsilon_L) | \bar{d}_\alpha(z) u_\beta(0) | 0 \rangle = \frac{1}{\sqrt{2N_c}} \int_0^1 e^{ixP \cdot z} \left\{ \not{\epsilon} \left[\not{p}_\rho \phi_\rho^t(x) + m_\rho \phi_\rho(x) \right] + m_\rho \phi_\rho^s(x) \right\} \quad (10)$$

The second term in the above equation is the leading twist wave function (twist-2), while the first and third terms are sub-leading twist (twist-3) wave functions.

The transverse momentum k^\perp is usually conveniently converted to the b parameter by Fourier transformation. The initial conditions of $\phi_i(x)$, $i = B, \pi$, are of non-perturbative origin, satisfying the normalization

$$\int_0^1 \phi_i(x, b=0) dx = \frac{1}{2\sqrt{6}} f_i, \quad (11)$$

with f_i the meson decay constants.

3 Perturbative Calculations

In the previous section we have discussed the wave functions and Wilson coefficients of the factorization formula in eq.(1). In this section, we will calculate the hard part $H(t)$. This part involves the four quark operators and the necessary hard gluon connecting the four quark operator and the spectator quark. Since the final results are expressed as integrations of the distribution function variables, we will show the whole amplitude for each diagram including wave functions.

Similar to the $B \rightarrow \pi\pi$ decays [10], there are 8 type diagrams contributing to the $B \rightarrow \pi\rho$ decays, which are shown in Figure 1. Let's first calculate the usual factorizable diagrams (a) and (b). Operators O_1, O_2, O_3, O_4, O_9 , and O_{10} are $(V-A)(V-A)$ currents, the sum of their amplitudes is given as

$$\begin{aligned} F_e = & 8\sqrt{2}\pi C_F G_F f_\rho m_\rho m_B^2 (\epsilon \cdot p_\pi) \int_0^1 dx_1 dx_2 \int_0^\infty b_1 db_1 b_2 db_2 \phi_B(x_1, b_1) \\ & \left\{ \left[(1+x_2) \phi_\pi^A(x_2, b_2) + r_\pi (1-2x_2) \left(\phi_\pi^P(x_2, b_2) + \phi_\pi^\sigma(x_2, b_2) \right) \right] \alpha_s(t_e^1) \right. \\ & h_e(x_1, x_2, b_1, b_2) \exp[-S_{ab}(t_e^1)] \\ & \left. + 2r_\pi \phi_\pi^P(x_2, b_2) \alpha_s(t_e^2) h_e(x_2, x_1, b_2, b_1) \exp[-S_{ab}(t_e^2)] \right\}, \end{aligned} \quad (12)$$

where $r_\pi = m_0/m_B = m_\pi^2/[m_B(m_u + m_d)]$; $C_F = 4/3$ is a color factor. The function h_e , the scales t_e^i and the Sudakov factors S_{ab} are displayed in the appendix. In the above equation, we do not include the Wilson coefficients of the corresponding operators, which are process dependent. They will be shown later in this section for different decay channels. The diagrams Fig.1(a)(b) are also the diagrams for the $B \rightarrow \pi$ form factor $F_1^{B \rightarrow \pi}$. Therefore we can extract $F_1^{B \rightarrow \pi}$ from eq.(12).

$$F_1^{B \rightarrow \pi}(q^2 = 0) = \frac{F_e}{\sqrt{2} G_F f_\rho m_\rho (\epsilon \cdot p_\pi)}. \quad (13)$$

The operators O_5 , O_6 , O_7 , and O_8 have a structure of $(V - A)(V + A)$. In some decay channels, some of these operators contribute to the decay amplitude in a factorizable way. Since only the vector part of the $(V+A)$ current contribute to the vector meson production,

$$\langle \pi | V - A | B \rangle \langle \rho | V + A | 0 \rangle = \langle \pi | V - A | B \rangle \langle \rho | V - A | 0 \rangle, \quad (14)$$

the result of these operators is the same as eq.(12). In some other cases, we need to do Fierz transformation for these operators to get right color structure for factorization to work. In this case, we get $(S-P)(S+P)$ operators from $(V-A)(V+A)$ ones. Because neither scalar nor pseudo-scalar density gives contribution to a vector meson production $\langle \rho | S + P | 0 \rangle = 0$, we get

$$F_e^P = 0. \quad (15)$$

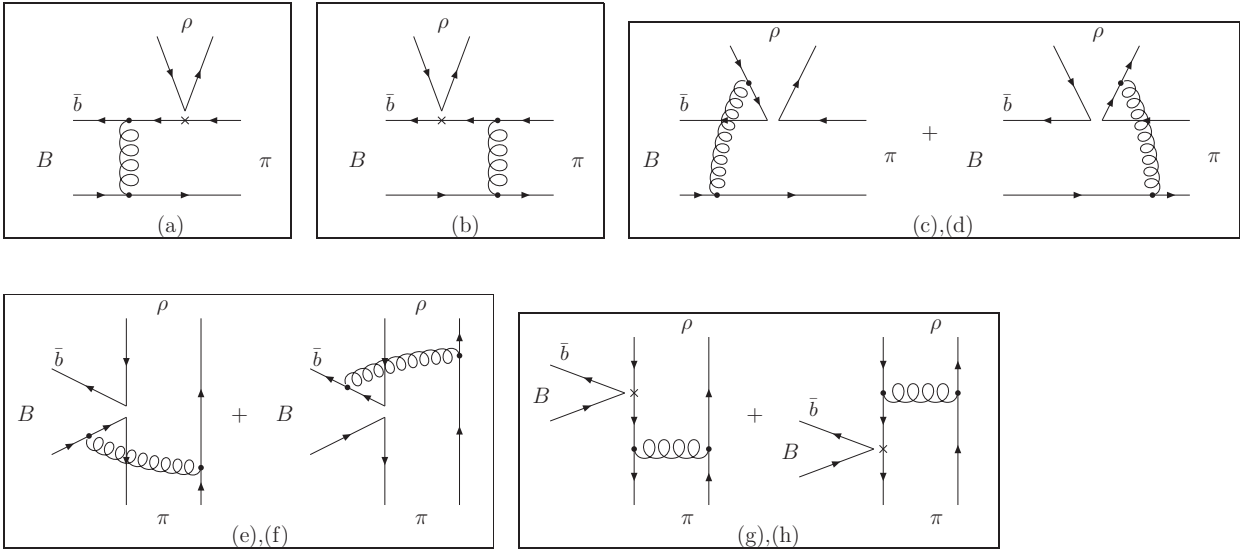


Figure 1: Diagrams contributing to the $B \rightarrow \pi \rho$ decays (diagram (a) and (b) contribute to the $B \rightarrow \pi$ form factor).

For the non-factorizable diagrams (c) and (d), all three meson wave functions are involved. The integration of b_3 can be performed easily using δ function $\delta(b_3 - b_1)$, leaving only integration of b_1 and b_2 . For the $(V - A)(V - A)$ operators the result is

$$M_e = -\frac{32}{3} \sqrt{3} \pi C_F G_F m_\rho m_B^2 (\epsilon \cdot p_\pi) \int_0^1 dx_1 dx_2 dx_3 \int_0^\infty b_1 db_1 b_2 db_2 \phi_B(x_1, b_1) x_2 \left[\phi_\pi^A(x_2, b_1) - 2r_\pi \phi_\pi^\sigma(x_2, b_1) \right] \phi_\rho(x_3, b_2) h_d(x_1, x_2, x_3, b_1, b_2) \exp[-S_{cd}(t_d)] . \quad (16)$$

For the $(V - A)(V + A)$ operators the formula is different,

$$\begin{aligned}
M_e^P = & \frac{64}{3} \sqrt{3} \pi C_F G_F m_\rho^2 m_B (\epsilon \cdot p_\pi) \int_0^1 dx_1 dx_2 dx_3 \int_0^\infty b_1 db_1 b_2 db_2 \phi_B(x_1, b_1) \times \\
& \left\{ r_\pi(x_3 - x_2) \left[\phi_\pi^P(x_2, b_1) \phi_\rho^t(x_3, b_2) + \phi_\pi^\sigma(x_2, b_1) \phi_\rho^s(x_3, b_2) \right] \right. \\
& - r_\pi(x_2 + x_3) \left[\phi_\pi^P(x_2, b_1) \phi_\rho^s(x_3, b_2) + \phi_\pi^\sigma(x_2, b_1) \phi_\rho^t(x_3, b_2) \right] \\
& \left. + x_3 \phi_\pi^A(x_2, b_1) \left[\phi_\rho^t(x_3, b_2) - \phi_\rho^s(x_3, b_2) \right] \right\} h_d(x_1, x_2, x_3, b_1, b_2) \exp[-S_{cd}(t_d)] . \quad (17)
\end{aligned}$$

Comparing with the expression of M_e in eq.(16), the $(V - A)(V + A)$ type result M_e^P is suppressed by m_ρ/m_B .

For the non-factorizable annihilation diagrams (e) and (f), again all three wave functions are involved. The integration of b_3 can be performed easily using $\delta(b_3 - b_2)$. Here we have two kind of contributions, which are different. M_a is contribution containing operator type $(V - A)(V - A)$, and M_a^P is contribution containing operator type $(V - A)(V + A)$.

$$\begin{aligned}
M_a = & \frac{32}{3} \sqrt{3} \pi C_F G_F m_\rho m_B^2 (\epsilon \cdot p_\pi) \int_0^1 dx_1 dx_2 dx_3 \int_0^\infty b_1 db_1 b_2 db_2 \phi_B(x_1, b_1) \times \\
& \left\{ \left[x_2 \phi_\pi^A(x_2, b_2) \phi_\rho(x_3, b_2) + r_\pi r_\rho (x_2 - x_3) \left(\phi_\pi^P(x_2, b_2) \phi_\rho^t(x_3, b_2) + \phi_\pi^\sigma(x_2, b_2) \phi_\rho^s(x_3, b_2) \right) \right. \right. \\
& \left. \left. + r_\pi r_\rho (x_2 + x_3) \left(\phi_\pi^\sigma(x_2, b_2) \phi_\rho^t(x_3, b_2) + \phi_\pi^P(x_2, b_2) \phi_\rho^s(x_3, b_2) \right) \right] \right. \\
& \times h_f^1(x_1, x_2, x_3, b_1, b_2) \exp[-S_{ef}(t_f^1)] \\
& - \left[x_3 \phi_\pi^A(x_2, b_2) \phi_\rho(x_3, b_2) + r_\pi r_\rho (x_3 - x_2) \left(\phi_\pi^P(x_2, b_2) \phi_\rho^t(x_3, b_2) + \phi_\pi^\sigma(x_2, b_2) \phi_\rho^s(x_3, b_2) \right) \right. \\
& \left. \left. + r_\pi r_\rho (2 + x_2 + x_3) \phi_\pi^P(x_2, b_2) \phi_\rho^s(x_3, b_2) - r_\pi r_\rho (2 - x_2 - x_3) \phi_\pi^\sigma(x_2, b_2) \phi_\rho^t(x_3, b_2) \right] \right. \\
& \left. h_f^2(x_1, x_2, x_3, b_1, b_2) \exp[-S_{ef}(t_f^2)] \right\} , \quad (18)
\end{aligned}$$

$$\begin{aligned}
M_a^P = & -\frac{32}{3} \sqrt{3} \pi C_F G_F m_\rho m_B^2 (\epsilon \cdot p_\pi) \int_0^1 dx_1 dx_2 dx_3 \int_0^\infty b_1 db_1 b_2 db_2 \phi_B(x_1, b_1) \times \\
& \left\{ \left[x_2 r_\pi \phi_\rho(x_3, b_2) \left(\phi_\pi^P(x_2, b_2) + \phi_\pi^\sigma(x_2, b_2) \right) - x_3 r_\rho \phi_\pi^A(x_2, b_2) \left(\phi_\rho^t(x_3, b_2) + \phi_\rho^s(x_3, b_2) \right) \right] \right. \\
& \times h_f^1(x_1, x_2, x_3, b_1, b_2) \exp[-S_{ef}(t_f^1)] \\
& \left. + \left[(2 - x_2) r_\pi \phi_\rho(x_3, b_2) \left(\phi_\pi^P(x_2, b_2) + \phi_\pi^\sigma(x_2, b_2) \right) \right. \right. \\
& \left. \left. - r_\rho (2 - x_3) \phi_\pi^A(x_2, b_2) \left(\phi_\rho^t(x_3, b_2) + \phi_\rho^s(x_3, b_2) \right) \right] h_f^2(x_1, x_2, x_3, b_1, b_2) \exp[-S_{ef}(t_f^2)] \right\} , \quad (19)
\end{aligned}$$

where $r_\rho = m_\rho/m_B$. The factorizable annihilation diagrams (g) and (h) involve only π and ρ wave functions. There are also two kinds of decay amplitudes for these two diagrams. F_a is for $(V - A)(V - A)$ type operators, and F_a^P is for $(S - P)(S + P)$ type operators.

$$F_a = 8\sqrt{2} C_F G_F \pi f_B m_\rho m_B^2 (\epsilon \cdot p_\pi) \int_0^1 dx_1 dx_2 \int_0^\infty b_1 db_1 b_2 db_2 \times$$

$$\begin{aligned}
& \left\{ \left[x_2 \phi_\pi^A(x_1, b_1) \phi_\rho(x_2, b_2) - 2(1 - x_2) r_\pi r_\rho \phi_\pi^P(x_1, b_1) \phi_\rho^t(x_2, b_2) \right. \right. \\
& \quad \left. \left. + 2(1 + x_2) r_\pi r_\rho \phi_\pi^P(x_1, b_1) \phi_\rho^s(x_2, b_2) \right] \alpha_s(t_e^1) h_a(x_2, x_1, b_2, b_1) \exp[-S_{gh}(t_e^1)] \right. \\
& \quad \left. - \left[x_1 \phi_\pi^A(x_1, b_1) \phi_\rho(x_2, b_2) + 2(1 + x_1) r_\pi r_\rho \phi_\pi^P(x_1, b_1) \phi_\rho^s(x_2, b_2) \right. \right. \\
& \quad \left. \left. - 2(1 - x_1) r_\pi r_\rho \phi_\pi^\sigma(x_1, b_1) \phi_\rho^s(x_2, b_2) \right] \alpha_s(t_e^2) h_a(x_1, x_2, b_1, b_2) \exp[-S_{gh}(t_e^2)] \right\} , \quad (20) \\
F_a^P &= 16\sqrt{2} C_F G_F \pi f_B m_\rho m_B^2 (\epsilon \cdot p_\pi) \int_0^1 dx_1 dx_2 \int_0^\infty b_1 db_1 b_2 db_2 \\
& \times \left\{ \left[2r_\pi \phi_\pi^P(x_1, b_1) \phi_\rho(x_2, b_2) + x_2 r_\rho \phi_\pi^A(x_1, b_1) \left(\phi_\rho^s(x_2, b_2) - \phi_\rho^t(x_2, b_2) \right) \right] \right. \\
& \quad \alpha_s(t_e^1) h_a(x_2, x_1, b_2, b_1) \exp[-S_{gh}(t_e^1)] \\
& \quad \left. + \left[x_1 r_\pi \left(\phi_\pi^P(x_1, b_1) - \phi_\pi^\sigma(x_1, b_1) \right) \phi_\rho(x_2, b_2) + 2r_\rho \phi_\pi^A(x_1, b_1) \phi_\rho^s(x_2, b_2) \right] \right. \\
& \quad \left. \alpha_s(t_e^2) h_a(x_1, x_2, b_1, b_2) \exp[-S_{gh}(t_e^2)] \right\} , \quad (21)
\end{aligned}$$

In the above equations, we have used the assumption that $x_1 \ll x_2, x_3$. Since the light quark momentum fraction x_1 in B meson is peaked at the small region, while quark momentum fraction x_2 of pion is peaked around 0.5, this is not a bad approximation. The numerical results also show that this approximation makes very little difference in the final result. After using this approximation, all the diagrams are functions of $k_1^- = x_1 m_B / \sqrt{2}$ of B meson only, independent of the variable of k_1^+ . Therefore the integration of eq.(7) is performed safely.

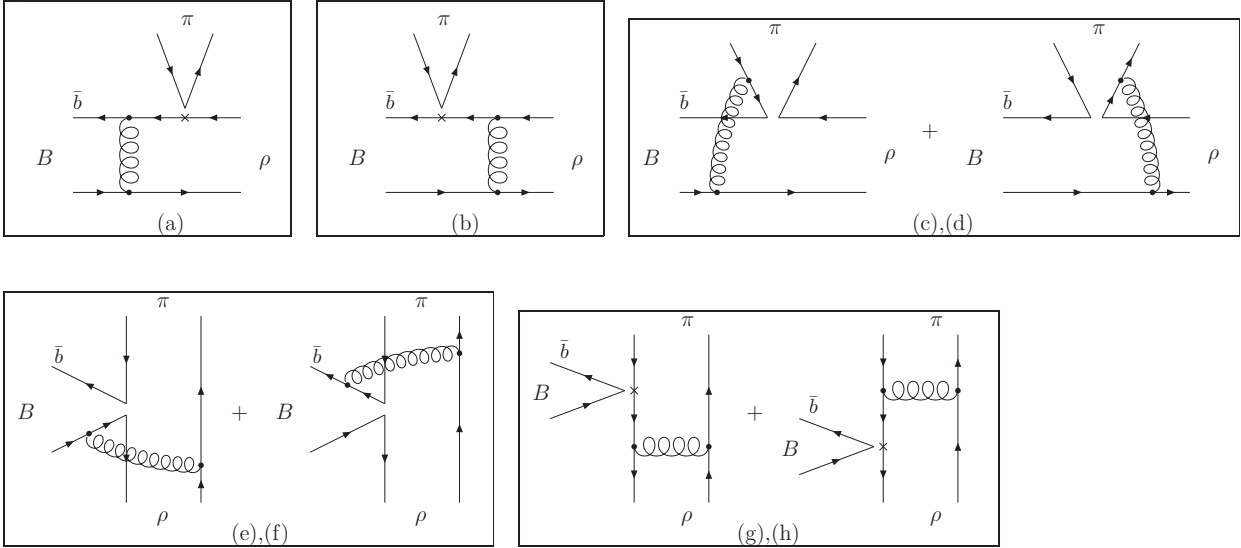


Figure 2: Diagrams contributing to the $B \rightarrow \pi \rho$ decays (diagram (a) and (b) contribute to the $B \rightarrow \rho$ form factor $A_0^{B \rightarrow \rho}$).

If we exchange the π and ρ in Figure 1, the result will be different for some diagrams.

Because this will switch the dominant contribution from $B \rightarrow \pi$ form factor to $B \rightarrow \rho$ form factor. The new diagrams are shown in Figure 2. Inserting $(V - A)(V - A)$ operators, the corresponding amplitude for Figure 2(a)(b) is

$$\begin{aligned}
F_{e\rho} = & 8\sqrt{2}\pi C_F G_F f_\pi m_\rho m_B^2 (\epsilon \cdot p_\pi) \int_0^1 dx_1 dx_2 \int_0^\infty b_1 db_1 b_2 db_2 \phi_B(x_1, b_1) \\
& \times \left\{ \left[(1+x_2)\phi_\rho(x_2, b_2) + (1-2x_2)r_\rho \left(\phi_\rho^t(x_2, b_2) + \phi_\rho^s(x_2, b_2) \right) \right] \right. \\
& \alpha_s(t_e^1) h_e(x_1, x_2, b_1, b_2) \exp[-S_{ab}(t_e^1)] \\
& \left. + 2r_\rho \phi_\rho^s(x_2, b_2) \alpha_s(t_e^2) h_e(x_2, x_1, b_2, b_1) \exp[-S_{ab}(t_e^2)] \right\}. \quad (22)
\end{aligned}$$

These two diagrams are also responsible for the calculation of $B \rightarrow \rho$ form factors. The form factor relative to the $B \rightarrow \pi\rho$ decays is $A_0^{B \rightarrow \rho}$, which can be extracted from eq.(22)

$$A_0^{B \rightarrow \rho}(q^2 = 0) = \frac{F_{e\rho}}{\sqrt{2}G_F f_\pi m_\rho (\epsilon \cdot p_\pi)}. \quad (23)$$

For $(V - A)(V + A)$ operators, Figure 2(a) and 2(b) give

$$\begin{aligned}
F_{e\rho}^P = & -16\sqrt{2}\pi C_F G_F f_\pi m_\rho r_\pi m_B^2 (\epsilon \cdot p_\pi) \int_0^1 dx_1 dx_2 \int_0^\infty b_1 db_1 b_2 db_2 \phi_B(x_1, b_1) \\
& \times \left\{ \left[\phi_\rho(x_2, b_2) - r_\rho x_2 \phi_\rho^t(x_2, b_2) + (2+x_2)r_\rho \phi_\rho^s(x_2, b_2) \right] \right. \\
& \times \alpha_s(t_e^1) h_e(x_1, x_2, b_1, b_2) \exp[-S_{ab}(t_e^1)] \\
& \left. + \left[x_1 \phi_\rho(x_2, b_2) + 2r_\rho \phi_\rho^s(x_2, b_2) \right] \alpha_s(t_e^2) h_e(x_2, x_1, b_2, b_1) \exp[-S_{ab}(t_e^2)] \right\}, \quad (24)
\end{aligned}$$

For the nonfactorizable diagrams Figure 2(c) and 2(d) the result is

$$\begin{aligned}
M_{e\rho} = & -\frac{32}{3}\sqrt{3}\pi C_F G_F m_\rho m_B^2 (\epsilon \cdot p_\pi) \int_0^1 dx_1 dx_2 dx_3 \int_0^\infty b_1 db_1 b_2 db_2 \phi_B(x_1, b_1) \\
& \times x_2 \left[\phi_\rho(x_2, b_2) - 2r_\rho \phi_\rho^t(x_2, b_2) \right] \phi_\pi^A(x_3, b_1) h_d(x_1, x_2, x_3, b_1, b_2) \exp[-S_{cd}(t_d)]. \quad (25)
\end{aligned}$$

For the nonfactorizable annihilation diagrams (e) and (f), we have $M_{a\rho}$ for $(V - A)(V - A)$ operators and $M_{a\rho}^P$ for $(V - A)(V + A)$ operators.

$$\begin{aligned}
M_{a\rho} = & \frac{32}{3}\sqrt{3}\pi C_F G_F m_\rho m_B^2 (\epsilon \cdot p_\pi) \int_0^1 dx_1 dx_2 dx_3 \int_0^\infty b_1 db_1 b_2 db_2 \phi_B(x_1, b_1) \left\{ \exp[-S_{ef}(t_f^1)] \right. \\
& \left[x_2 \phi_\pi^A(x_3, b_2) \phi_\rho(x_2, b_2) + r_\pi r_\rho (x_2 - x_3) \left(\phi_\pi^P(x_3, b_2) \phi_\rho^t(x_2, b_2) + \phi_\pi^\sigma(x_3, b_2) \phi_\rho^s(x_2, b_2) \right) \right. \\
& \left. + r_\pi r_\rho (x_2 + x_3) \left(\phi_\pi^\sigma(x_3, b_2) \phi_\rho^t(x_2, b_2) + \phi_\pi^P(x_3, b_2) \phi_\rho^s(x_2, b_2) \right) \right] h_f^1(x_1, x_2, x_3, b_1, b_2) \\
& - \left[x_3 \phi_\pi^A(x_3, b_2) \phi_\rho(x_2, b_2) + r_\pi r_\rho (x_3 - x_2) \left(\phi_\pi^P(x_3, b_2) \phi_\rho^t(x_2, b_2) + \phi_\pi^\sigma(x_3, b_2) \phi_\rho^s(x_2, b_2) \right) \right. \\
& \left. \left. - r_\pi r_\rho (2 - x_2 - x_3) \phi_\pi^\sigma(x_3, b_2) \phi_\rho^t(x_2, b_2) + r_\pi r_\rho (2 + x_2 + x_3) \phi_\pi^P(x_3, b_2) \phi_\rho^s(x_2, b_2) \right] \right\}
\end{aligned}$$

$$h_f^2(x_1, x_2, x_3, b_1, b_2) \exp[-S_{ef}(t_f^2)] \} , \quad (26)$$

$$M_{a\rho}^P = M_a^P , \quad (27)$$

For the factorizable annihilation diagrams (g) and (h)

$$F_{a\rho} = -F_a, \quad (28)$$

$$F_{a\rho}^P = -F_a^P , \quad (29)$$

If the ρ meson replaced by ω meson in Figure 1 and 2, the formulas will be the same, except replacing f_ρ by f_ω and ϕ_ρ replaced by ϕ_ω .

In the language of the above matrix elements for different diagrams eq.(12-29,), the decay amplitude for $B^0 \rightarrow \pi^+ \rho^-$ can be written as

$$\begin{aligned} \mathcal{M}(B^0 \rightarrow \pi^+ \rho^-) &= F_{e\rho} \left[\xi_u \left(\frac{1}{3} C_1 + C_2 \right) - \xi_t \left(C_4 + \frac{1}{3} C_3 + C_{10} + \frac{1}{3} C_9 \right) \right] \\ &- F_{e\rho}^P \xi_t \left[C_6 + \frac{1}{3} C_5 + C_8 + \frac{1}{3} C_7 \right] \\ &+ M_{e\rho} [\xi_u C_1 - \xi_t (C_3 + C_9)] \\ &+ M_a \left[\xi_u C_2 - \xi_t \left(C_4 - C_6 + \frac{1}{2} C_8 + C_{10} \right) \right] \\ &- M_{a\rho} \xi_t \left[C_3 + C_4 - C_6 - C_8 - \frac{1}{2} C_9 - \frac{1}{2} C_{10} \right] \\ &- M_{a\rho}^P \xi_t \left[C_5 - \frac{1}{2} C_7 \right] + F_a \left[\xi_u \left(C_1 + \frac{1}{3} C_2 \right) \right. \\ &\quad \left. - \xi_t \left(-\frac{1}{3} C_3 - C_4 - \frac{3}{2} C_7 - \frac{1}{2} C_8 + \frac{5}{3} C_9 + C_{10} \right) \right] \\ &+ F_a^P \xi_t \left[\frac{1}{3} C_5 + C_6 - \frac{1}{6} C_7 - \frac{1}{2} C_8 \right] . \end{aligned} \quad (30)$$

where $\xi_u = V_{ub}^* V_{ud}$, $\xi_t = V_{tb}^* V_{td}$. The C_i 's should be calculated at the appropriate scale t using equations in the appendices of ref.[10]. The decay amplitude of the charge conjugate decay channel $\bar{B}^0 \rightarrow \rho^+ \pi^-$ is the same as eq.(30) except replacing the CKM matrix elements ξ_u to ξ_u^* and ξ_t to ξ_t^* under the definition of charge conjugation $C|B^0\rangle = -|\bar{B}^0\rangle$.

$$\begin{aligned} \mathcal{M}(B^0 \rightarrow \rho^+ \pi^-) &= F_e \left[\xi_u \left(\frac{1}{3} C_1 + C_2 \right) - \xi_t \left(C_4 + \frac{1}{3} C_3 + C_{10} + \frac{1}{3} C_9 \right) \right] \\ &+ M_e [\xi_u C_1 - \xi_t (C_3 + C_9)] - M_e^P \xi_t [C_5 + C_7] \\ &+ M_{a\rho} \left[\xi_u C_2 - \xi_t \left(C_4 - C_6 + \frac{1}{2} C_8 + C_{10} \right) \right] \end{aligned}$$

$$\begin{aligned}
& - M_a \xi_t \left[C_3 + C_4 - C_6 - C_8 - \frac{1}{2}C_9 - \frac{1}{2}C_{10} \right] \\
& - M_a^P \xi_t \left[C_5 - \frac{1}{2}C_7 \right] + F_a \left[\xi_u \left(-C_1 - \frac{1}{3}C_2 \right) \right. \\
& \quad \left. - \xi_t \left(\frac{1}{3}C_3 + C_4 + \frac{3}{2}C_7 + \frac{1}{2}C_8 - \frac{5}{3}C_9 - C_{10} \right) \right] \\
& - F_a^P \xi_t \left[\frac{1}{3}C_5 + C_6 - \frac{1}{6}C_7 - \frac{1}{2}C_8 \right].
\end{aligned} \tag{31}$$

The decay amplitude for $B^0 \rightarrow \pi^0 \rho^0$ can be written as

$$\begin{aligned}
-2\mathcal{M}(B^0 \rightarrow \pi^0 \rho^0) &= F_e \left[\xi_u \left(C_1 + \frac{1}{3}C_2 \right) \right. \\
& - \xi_t \left(-\frac{1}{3}C_3 - C_4 + \frac{3}{2}C_7 + \frac{1}{2}C_8 + \frac{5}{3}C_9 + C_{10} \right) \Big] \\
& + F_{e\rho} \left[\xi_u \left(C_1 + \frac{1}{3}C_2 \right) \right. \\
& - \xi_t \left(-\frac{1}{3}C_3 - C_4 - \frac{3}{2}C_7 - \frac{1}{2}C_8 + \frac{5}{3}C_9 + C_{10} \right) \Big] \\
& + F_{e\rho}^P \xi_t \left[\frac{1}{3}C_5 + C_6 - \frac{1}{6}C_7 - \frac{1}{2}C_8 \right] \\
& + M_e \left[\xi_u C_2 - \xi_t \left(-C_3 - \frac{3}{2}C_8 + \frac{1}{2}C_9 + \frac{3}{2}C_{10} \right) \right] \\
& + M_{e\rho} \left[\xi_u C_2 - \xi_t \left(-C_3 + \frac{3}{2}C_8 + \frac{1}{2}C_9 + \frac{3}{2}C_{10} \right) \right] \\
& - (M_a + M_{a\rho}) \left[\xi_u C_2 \right. \\
& \quad \left. - \xi_t \left(C_3 + 2C_4 - 2C_6 - \frac{1}{2}C_8 - \frac{1}{2}C_9 + \frac{1}{2}C_{10} \right) \right] \\
& + (M_e^P + 2M_a^P) \xi_t \left[C_5 - \frac{1}{2}C_7 \right].
\end{aligned} \tag{32}$$

The decay amplitude for $B^+ \rightarrow \rho^+ \pi^0$ can be written as

$$\begin{aligned}
\sqrt{2}\mathcal{M}(B^+ \rightarrow \rho^+ \pi^0) &= (F_e + 2F_a) \left[\xi_u \left(\frac{1}{3}C_1 + C_2 \right) - \xi_t \left(\frac{1}{3}C_3 + C_4 + C_{10} + \frac{1}{3}C_9 \right) \right] \\
& + F_{e\rho} \left[\xi_u \left(C_1 + \frac{1}{3}C_2 \right) - \xi_t \left(-\frac{1}{3}C_3 - C_4 - \frac{3}{2}C_7 - \frac{1}{2}C_8 + C_{10} + \frac{5}{3}C_9 \right) \right] \\
& - F_{e\rho}^P \xi_t \left[-\frac{1}{3}C_5 - C_6 + \frac{1}{2}C_8 + \frac{1}{6}C_7 \right] \\
& + M_{e\rho} \left[\xi_u C_2 - \xi_t \left(-C_3 + \frac{3}{2}C_8 + \frac{1}{2}C_9 + \frac{3}{2}C_{10} \right) \right] \\
& + (M_e + M_a - M_{a\rho}) \left[\xi_u C_1 - \xi_t (C_3 + C_9) \right] \\
& - M_e^P \xi_t [C_5 + C_7] - 2F_a^P \xi_t \left[\frac{1}{3}C_5 + C_6 + \frac{1}{3}C_7 + C_8 \right].
\end{aligned} \tag{33}$$

The decay amplitude for $B^+ \rightarrow \pi^+ \rho^0$ can be written as

$$\sqrt{2}\mathcal{M}(B^+ \rightarrow \pi^+ \rho^0) = F_e \left[\xi_u \left(C_1 + \frac{1}{3}C_2 \right) \right]$$

$$\begin{aligned}
& -\xi_t \left(-\frac{1}{3}C_3 - C_4 + \frac{3}{2}C_7 + \frac{1}{2}C_8 + \frac{5}{3}C_9 + C_{10} \right) \Big] \\
& + (F_{e\rho} - 2F_a) \left[\xi_u \left(\frac{1}{3}C_1 + C_2 \right) - \xi_t \left(\frac{1}{3}C_3 + C_4 + \frac{1}{3}C_9 + C_{10} \right) \right] \\
& - (F_{e\rho}^P - 2F_a^P) \xi_t \left[\frac{1}{3}C_5 + C_6 + \frac{1}{3}C_7 + C_8 \right] \\
& + M_e \left[\xi_u C_2 - \xi_t \left(-C_3 - \frac{3}{2}C_8 + \frac{1}{2}C_9 + \frac{3}{2}C_{10} \right) \right] \\
& + (M_{e\rho} - M_a + M_{a\rho}) [\xi_u C_1 - \xi_t (C_3 + C_9)] \\
& + M_e^P \xi_t \left[C_5 - \frac{1}{2}C_7 \right]. \tag{34}
\end{aligned}$$

From eq.(30-34), we can verify that the isospin relation

$$\begin{aligned}
& \mathcal{M}(B^0 \rightarrow \pi^+ \rho^-) + \mathcal{M}(B^0 \rightarrow \pi^- \rho^+) - 2\mathcal{M}(B^0 \rightarrow \pi^0 \rho^0) \\
& = \sqrt{2}\mathcal{M}(B^+ \rightarrow \pi^0 \rho^+) + \sqrt{2}\mathcal{M}(B^+ \rightarrow \pi^+ \rho^0), \tag{35}
\end{aligned}$$

holds exactly in our calculations.

The decay amplitude for $B^+ \rightarrow \pi^+ \omega$ can also be written as expressions of the above F_i and M_i , but remember replacing f_ρ by f_ω and ϕ_ρ by ϕ_ω .

$$\begin{aligned}
\sqrt{2}\mathcal{M}(B^+ \rightarrow \pi^+ \omega) & = F_e \left[\xi_u \left(C_1 + \frac{1}{3}C_2 \right) \right. \\
& \quad \left. - \xi_t \left(\frac{7}{3}C_3 + \frac{5}{3}C_4 + 2C_5 + \frac{2}{3}C_6 + \frac{1}{2}C_7 + \frac{1}{6}C_8 + \frac{1}{3}C_9 - \frac{1}{3}C_{10} \right) \right] \\
& + F_{e\rho} \left[\xi_u \left(\frac{1}{3}C_1 + C_2 \right) - \xi_t \left(\frac{1}{3}C_3 + C_4 + \frac{1}{3}C_9 + C_{10} \right) \right] \\
& - F_{e\rho}^P \xi_t \left[\frac{1}{3}C_5 + C_6 + \frac{1}{3}C_7 + C_8 \right] \\
& + M_e \left[\xi_u C_2 - \xi_t \left(C_3 + 2C_4 - 2C_6 - \frac{1}{2}C_8 - \frac{1}{2}C_9 + \frac{1}{2}C_{10} \right) \right] \\
& + (M_{e\rho} + M_a + M_{a\rho}) [\xi_u C_1 - \xi_t (C_3 + C_9)] \\
& - (M_a^P + M_{a\rho}^P) \xi_t [C_5 + C_7] - M_e^P \xi_t \left[C_5 - \frac{1}{2}C_7 \right]. \tag{36}
\end{aligned}$$

The decay amplitude for $B^0 \rightarrow \pi^0 \omega$ can be written as

$$\begin{aligned}
2\mathcal{M}(B^0 \rightarrow \pi^0 \omega) & = F_e \left[\xi_u \left(-C_1 - \frac{1}{3}C_2 \right) \right. \\
& \quad \left. - \xi_t \left(-\frac{7}{3}C_3 - \frac{5}{3}C_4 - 2C_5 - \frac{2}{3}C_6 - \frac{1}{2}C_7 - \frac{1}{6}C_8 - \frac{1}{3}C_9 + \frac{1}{3}C_{10} \right) \right] \\
& + F_{e\rho} \left[\xi_u \left(C_1 + \frac{1}{3}C_2 \right) \right.
\end{aligned}$$

$$\begin{aligned}
& - \xi_t \left(-\frac{1}{3}C_3 - C_4 - \frac{3}{2}C_7 - \frac{1}{2}C_8 + \frac{5}{3}C_9 + C_{10} \right) \Big] \\
& + F_{e\rho}^P \xi_t \left[C_6 + \frac{1}{3}C_5 - \frac{1}{6}C_7 - \frac{1}{2}C_8 \right] \\
& + M_e \left[-\xi_u C_2 - \xi_t (-C_3 - 2C_4 + 2C_6 + \frac{1}{2}C_8 + \frac{1}{2}C_9 - \frac{1}{2}C_{10}) \right] \\
& + M_{e\rho} \left[\xi_u C_2 - \xi_t (-C_3 + \frac{3}{2}C_8 + \frac{1}{2}C_9 + \frac{3}{2}C_{10}) \right] \\
& + (M_a + M_{a\rho}) \left[\xi_u C_2 - \xi_t \left(-C_3 - \frac{3}{2}C_8 + \frac{1}{2}C_9 + \frac{3}{2}C_{10} \right) \right] \\
& + (M_e^P + 2M_a^P) \xi_t \left[C_5 - \frac{1}{2}C_7 \right].
\end{aligned} \tag{37}$$

4 Numerical calculations and discussions of Results

In the numerical calculations we use

$$\begin{aligned}
\Lambda_{\overline{\text{MS}}}^{(f=4)} &= 0.25 \text{GeV}, f_\pi = 130 \text{MeV}, f_B = 190 \text{MeV}, \\
m_0 &= 1.4 \text{GeV}, f_\rho = f_\omega = 200 \text{MeV}, f_\rho^T = f_\omega^T = 160 \text{MeV}, \\
M_B &= 5.2792 \text{GeV}, M_W = 80.41 \text{GeV}.
\end{aligned} \tag{38}$$

Note, for simplicity, we use the same value for f_ρ (f_ρ^T) and f_ω (f_ω^T). And this also makes it easy for us to see the major difference for the two mesons in the B decays. In principal, the decay constants can be a little different. For the light meson wave function, we neglect the b dependence part, which is not important in numerical analysis. We use wave function for ϕ_π^A and the twist-3 wave functions ϕ_π^P and ϕ_π^t from [16]

$$\phi_\pi^A(x) = \frac{3}{\sqrt{6}} f_\pi x(1-x) \left[1 + 0.44 C_2^{3/2}(2x-1) + 0.25 C_4^{3/2}(2x-1) \right], \tag{39}$$

$$\phi_\pi^P(x) = \frac{f_\pi}{2\sqrt{6}} \left[1 + 0.43 C_2^{1/2}(2x-1) + 0.09 C_4^{1/2}(2x-1) \right], \tag{40}$$

$$\phi_\pi^t(x) = \frac{f_\pi}{2\sqrt{6}} (1-2x) \left[1 + 0.55(10x^2 - 10x + 1) \right]. \tag{41}$$

The Gegenbauer polynomials are defined by

$$\begin{aligned}
C_2^{1/2}(t) &= \frac{1}{2}(3t^2 - 1), \quad C_4^{1/2}(t) = \frac{1}{8}(35t^4 - 30t^2 + 3), \\
C_2^{3/2}(t) &= \frac{3}{2}(5t^2 - 1), \quad C_4^{3/2}(t) = \frac{15}{8}(21t^4 - 14t^2 + 1),
\end{aligned} \tag{42}$$

whose coefficients correspond to $m_0 = 1.4$ GeV. In $B \rightarrow \pi\rho$, $\pi\omega$ decays, it is the longitudinal polarization of the ρ and ω meson contribute to the decay amplitude. Therefore we choose the wave function of ρ and ω meson similar to the pion case in eq.(39,41) [17]

$$\phi_\rho(x) = \phi_\omega(x) = \frac{3}{\sqrt{6}} f_\rho x(1-x) \left[1 + 0.18 C_2^{3/2} (2x-1) \right], \quad (43)$$

$$\begin{aligned} \phi_\rho^t(x) = \phi_\omega^t(x) = \frac{f_\rho^T}{2\sqrt{6}} \left\{ 3(2x-1)^2 + 0.3(2x-1)^2 [5(2x-1)^2 - 3] \right. \\ \left. + 0.21[3 - 30(2x-1)^2 + 35(2x-1)^4] \right\}, \end{aligned} \quad (44)$$

$$\phi_\rho^s(x) = \phi_\omega^s(x) = \frac{3}{2\sqrt{6}} f_\rho^T (1-2x) \left[1 + 0.76(10x^2 - 10x + 1) \right]. \quad (45)$$

Here again, for simplicity, we use the same expression for ρ and ω mesons.

For B meson, the wave function is chosen as

$$\phi_B(x, b) = \frac{N_B}{2\sqrt{6}} f_B x^2 (1-x)^2 \exp \left[-\frac{M_B^2 x^2}{2\omega_b^2} - \frac{1}{2} (\omega_b b)^2 \right], \quad (46)$$

with $\omega_b = 0.4$ GeV. $N_B = 2365.57$ is a normalization factor. We include full expression of twist-3 wave functions for light mesons unlike $B \rightarrow \pi\pi$ decays [10]. The twist-3 wave functions are also adopted from QCD sum rule calculations [16]. These changes make the $B \rightarrow \rho$ form factor a little larger than the $B \rightarrow \pi$ form factor [13]. However, this set of parameters does not change the $B^0 \rightarrow \pi^+\pi^-$ branching ratios. And we will see later that, this set of parameters will give good results of $B \rightarrow \pi\rho$ and $\pi\omega$ decays. With the above chosen wave functions, we get the corresponding form factors at zero momentum transfer from eq.(13,23):

$$F_0^{B \rightarrow \pi} = 0.30, \quad A_0^{B \rightarrow \rho} = 0.37.$$

They are close to the light cone QCD sum rule results [18].

The CKM parameters we used here are [19]

$$\begin{aligned} |V_{ud}| &= 0.9735 \pm 0.0008 & |V_{ub}/V_{cb}| &= 0.090 \pm 0.025 \\ |V_{cb}| &= 0.0405 \pm 0.0019 & |V_{tb}^* V_{td}| &= 0.0083 \pm 0.0016. \end{aligned} \quad (47)$$

We leave the CKM angle ϕ_2 as a free parameter. ϕ_2 's definition is

$$\phi_2 = \arg \left[-\frac{V_{td} V_{tb}^*}{V_{ud} V_{ub}^*} \right]. \quad (48)$$

In this parameterization, the decay amplitude of $B \rightarrow \pi\rho$ (or $\pi\omega$) can be rewritten as

$$\begin{aligned}\mathcal{M} &= V_{ub}^* V_{ud} T - V_{tb}^* V_{td} P \\ &= V_{ub}^* V_{ud} T \left[1 + z e^{i(\phi_2 + \delta)} \right],\end{aligned}\quad (49)$$

where $z = \left| \frac{V_{tb}^* V_{td}}{V_{ub}^* V_{ud}} \right| \left| \frac{P}{T} \right|$, and δ is the relative strong phase between tree (T) diagrams and penguin diagrams (P). z and δ can be calculated from PQCD. The corresponding charge conjugate decay mode is then

$$\begin{aligned}\overline{\mathcal{M}} &= V_{ub} V_{ud}^* T - V_{tb} V_{td}^* P \\ &= V_{ub} V_{ud}^* T \left[1 + z e^{i(-\phi_2 + \delta)} \right].\end{aligned}\quad (50)$$

Therefore the averaged branching ratio for $B \rightarrow \pi\rho$ is

$$\begin{aligned}Br &= (|\mathcal{M}|^2 + |\overline{\mathcal{M}}|^2)/2 \\ &= |V_{ub} V_{ud}^* T|^2 \left[1 + 2z \cos \phi_2 \cos \delta + z^2 \right],\end{aligned}\quad (51)$$

where $z = \left| \frac{V_{tb} V_{td}^*}{V_{ub} V_{ud}^*} \right| \left| \frac{P}{T} \right|$. Eq.(51) shows that the averaged branching ratio is a function of $\cos \phi_2$. This gives potential method to determine the CKM angle ϕ_2 by measuring only the averaged non-leptonic decay branching ratios. In our PQCD approach, the branching ratios and also the other quantities in eq.(51) are all calculable, such that $\cos \phi_2$ is measurable. However, there are still uncertainties in the input parameters of our approach as discussions below. More experimental data from BABAR and Belle can restrict these parameters in the near future.

More complicated, there are four decay channels of $B^0/\bar{B}^0 \rightarrow \pi^+ \rho^-$, $B^0/\bar{B}^0 \rightarrow \rho^+ \pi^-$. Due to $B\bar{B}$ mixing, it is very difficult to distinguish B^0 from \bar{B}^0 . But it is very easy to identify the final states. Therefore we sum up $B^0/\bar{B}^0 \rightarrow \pi^+ \rho^-$ as one channel, and $B^0/\bar{B}^0 \rightarrow \rho^+ \pi^-$ as another, although the summed up channels are not charge conjugate states. We show the branching ratio of $B^0/\bar{B}^0 \rightarrow \pi^+ \rho^-$, $B^0/\bar{B}^0 \rightarrow \rho^+ \pi^-$, $B^+ \rightarrow \pi^+ \rho^0$, $B^+ \rightarrow \rho^+ \pi^0$, and $B^+ \rightarrow \pi^+ \omega$ decays as a function of ϕ_2 in Figure 3. The branching ratio of $B^0/\bar{B}^0 \rightarrow \pi^+ \rho^-$ is a little larger than that of $B^0/\bar{B}^0 \rightarrow \pi^- \rho^+$ decays. Each of them is a sum of two decay channels. They are all getting larger when ϕ_2 is larger. The average of the two is in agreement with the recently measured branching ratios by CLEO [1] and BABAR [20]

$$\text{Br}(B^0 \rightarrow \pi^+ \rho^- + \pi^- \rho^+) = 27.6_{-7.4}^{+8.4} \pm 4.2 \times 10^{-6}, \quad \text{CLEO} \quad (52)$$

$$\text{Br}(B^0 \rightarrow \pi^+ \rho^- + \pi^- \rho^+) = 28.9 \pm 5.4 \pm 4.3 \times 10^{-6}, \quad \text{BABAR} \quad (53)$$

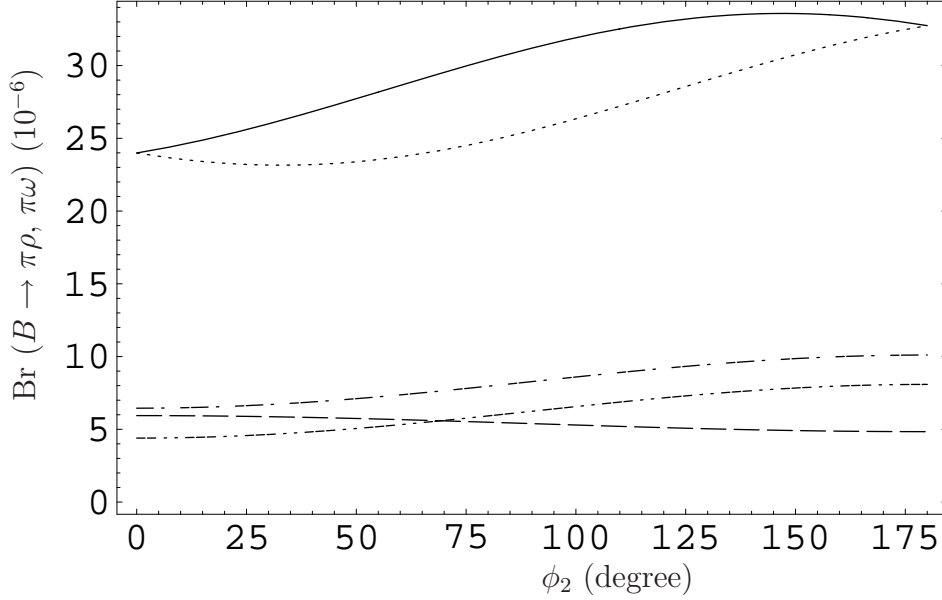


Figure 3: Branching ratios (10^{-6}) of $B^0/\bar{B}^0 \rightarrow \pi^+\rho^-$ (solid line), $B^0/\bar{B}^0 \rightarrow \rho^+\pi^-$ (dotted line), $B^+ \rightarrow \pi^+\rho^0$ (dashed line), $B^+ \rightarrow \rho^+\pi^0$ (dash-dotted line), and $B^+ \rightarrow \pi^+\omega$ (dash-dotted-dotted line), as a function of CKM angle ϕ_2 .

There are still large uncertainties in the experimental results. Therefore it is still early to fully determine the input parameters and to tell the CKM angle ϕ_2 from experiments.

The most uncertain parameters in our approach are from the meson wave functions. In principal, they can be only restricted by experiments, namely, semi-leptonic and non-leptonic decays of B mesons. Our parameters chosen for the numerical calculations in eq.(38,46) are best fit values from $B \rightarrow \pi\pi$ decays [10], $B \rightarrow \pi K$ [14], $B \rightarrow \pi$, $B \rightarrow \rho$ semi-leptonic decays [13] and some other experiments. As in these decays, we show the ω_b dependence of Branching ratios $Br(B^0/\bar{B}^0 \rightarrow \pi^\pm \rho^\mp)$ in Figure 4. The dotted, dashed and dash-dotted lines are for $\omega_b = 0.36$, 0.40 and 0.44, respectively. They are also shown as a function of CKM angle ϕ_2 . The two horizontal lines in the figure are BABAR measurements of 1σ . From the figure, we can see that the branching ratio is quite sensitive to the ω_b parameter. Fortunately, this parameter is also restricted from semi-leptonic decays [13]. In the near future, it will not be a big problem for us.

In Figure 5, we show the branching ratio of $B^0/\bar{B}^0 \rightarrow \pi^\pm \rho^\mp$ decays: $m_0 = 1.3$ GeV (dotted line), $m_0 = 1.4$ GeV (dashed line) and $m_0 = 1.5$ GeV (dash-dotted line) as a function of

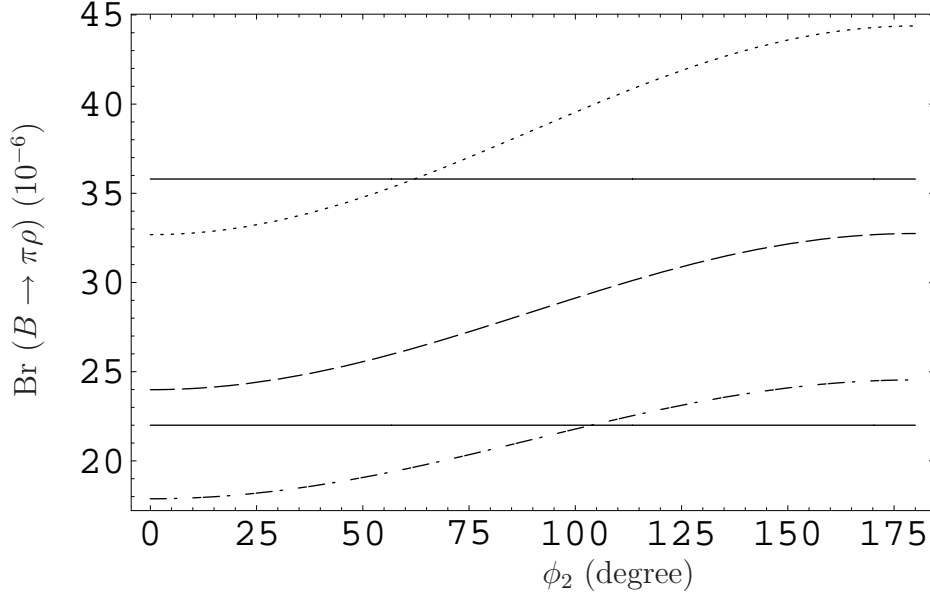


Figure 4: Branching ratios of $B^0/\bar{B}^0 \rightarrow \pi^\pm \rho^\mp$ decays: $\omega_b = 0.36$ (dotted line), $\omega_b = 0.40$ (dashed line) and $\omega_b = 0.44$ (dash-dotted line) as a function of CKM angle ϕ_2 . The two horizontal lines are BABAR measurements.

CKM angle ϕ_2 . m_0 is a parameter characterize the relative size of twist 3 contribution from twist 2 contribution. It originates from the Chiral perturbation theory and have a value near 1 GeV. Because of the Chiral enhancement of m_0 , the twist 3 contribution is at the same order magnitude as the twist 2 contribution. Thus the branching ratios of $Br(B^0/\bar{B}^0 \rightarrow \pi^\pm \rho^\mp)$ are also sensitive to this parameter, but not as strong as the ω_b dependence.

The branching ratios of $B^+ \rightarrow \pi^+ \rho^0$ and $B^+ \rightarrow \pi^+ \omega$ have little dependence on ϕ_2 . They are a little smaller than the CLEO measurement [1] showed below, but still within experimental error-bars.

$$\text{Br}(B^+ \rightarrow \pi^+ \rho^0) = 10.4_{-3.4}^{+3.3} \pm 2.1 \times 10^{-6}, \quad (54)$$

$$\text{Br}(B^+ \rightarrow \pi^+ \omega) = 11.3_{-2.9}^{+3.3} \pm 1.4 \times 10^{-6}. \quad (55)$$

However, the recent BABAR measurement is in good agreement with our prediction for $B^+ \rightarrow \pi^+ \omega$ [21]

$$\text{Br}(B^+ \rightarrow \pi^+ \omega) = 6.6_{-1.8}^{+2.1} \pm 0.7 \times 10^{-6}, \quad (56)$$

where the error-bars are also smaller. The preliminary result of Belle shows that the branching ratio of $B^+ \rightarrow \pi^+ \rho^0$ is around 6×10^{-6} [22]. This agrees with our prediction in Figure 3.

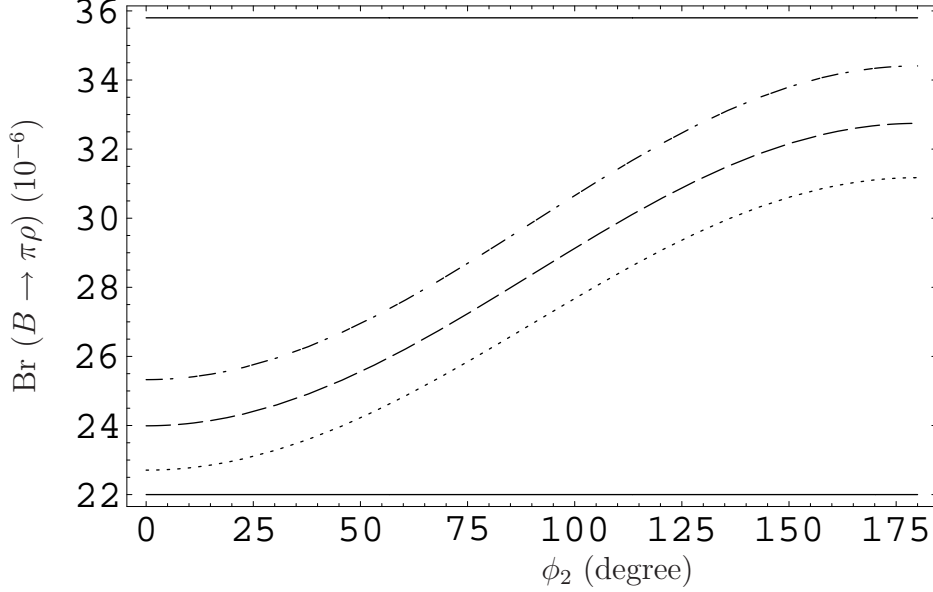


Figure 5: Branching ratios of $B^0/\bar{B}^0 \rightarrow \pi^\pm \rho^\mp$ decays: $m_0 = 1.3$ GeV (dotted line), $m_0 = 1.4$ GeV (dashed line) and $m_0 = 1.5$ GeV (dash-dotted line) as a function of CKM angle ϕ_2 . The two horizontal lines are BABAR measurements.

The averaged branching ratios of $B^0 \rightarrow \pi^0 \rho^0$ and $\pi^0 \omega$ are shown in Fig.6. They also have a large dependence on ϕ_2 . The behavior of them is quite different, due to the different isospin of ρ^0 and ω . But their branching ratios are rather small around 10^{-7} . They may not be measured in the current running B factories, but may be possible in the future experiments, like LHC-B and NLC. The recent BABAR upper limit of the channel is [20]

$$Br(B^0 \rightarrow \pi^0 \rho^0) < 10.6 \times 10^{-6}. \quad (57)$$

This is still consistent with our predictions in standard model (SM).

Using eq.(49-50), we can derive the direct CP violating parameter as

$$\begin{aligned} A_{CP}^{dir} &= \frac{|\mathcal{M}|^2 - |\overline{\mathcal{M}}|^2}{|\mathcal{M}|^2 + |\overline{\mathcal{M}}|^2} \\ &= \frac{2 \sin \phi_2 \sin \delta}{1 + 2z \cos \phi_2 \cos \delta + z^2}. \end{aligned} \quad (58)$$

Unsurprisingly, it is a function of $\cos \phi_2$ and $\sin \phi_2$. They are calculable in our PQCD approach. The direct CP violation parameters as a function of ϕ_2 are shown in figure 7. The direct CP violation parameter of $B^+ \rightarrow \pi^+ \rho^0$ and $B^0 \rightarrow \pi^0 \rho^0$ are positive and very large. While the direct CP violation parameter of $B^+ \rightarrow \rho^+ \pi^0$ and $B^0 \rightarrow \pi^0 \omega$ are negative and very large. The

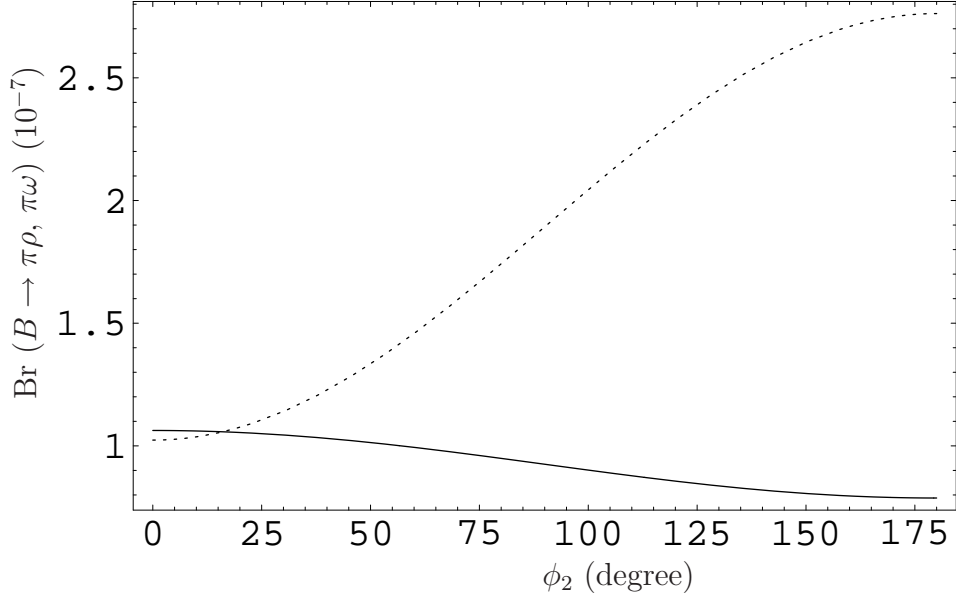


Figure 6: Branching ratios (10^{-7}) of $B^0 \rightarrow \pi^0 \rho^0$ (solid line), $B^0 \rightarrow \pi^0 \omega$ (dotted line), as a function of CKM angle ϕ_2 .

large strong phase required by the large direct CP asymmetry is from the non-factorizable and annihilation type diagrams, especially the annihilation diagrams. This is the different situation in Factorization approach where the main contribution comes from BSS mechanism [23] and the annihilation diagram has been neglected [24]. The direct CP violation of $B^+ \rightarrow \pi^+ \omega$ is rather small, since the annihilation diagram contributions in this decay is almost canceled out in eq.(36). The preliminary measurement of CLEO shows a large CP asymmetry for this decay [25]

$$A_{CP}(B^+ \rightarrow \pi^+ \omega) = 34 \pm 25\%. \quad (59)$$

Although the sign of CP is in agreement with our prediction, the central value is too large. If the result of central value remains in future experiments, we may expect new physics contributions.

For the neutral B^0 decays, there is more complication from the $B^0 \bar{B}^0$ mixing. The CP asymmetry is time dependent [24]:

$$A_{CP}(t) \simeq A_{CP}^{dir} \cos(\Delta m t) + a_{\epsilon+\epsilon'} \sin(\Delta m t), \quad (60)$$

where Δm is the mass difference of the two mass eigenstates of neutral B meson. The direct CP violation parameter A_{CP}^{dir} has already been defined in eq.(58). While the mixing-related CP

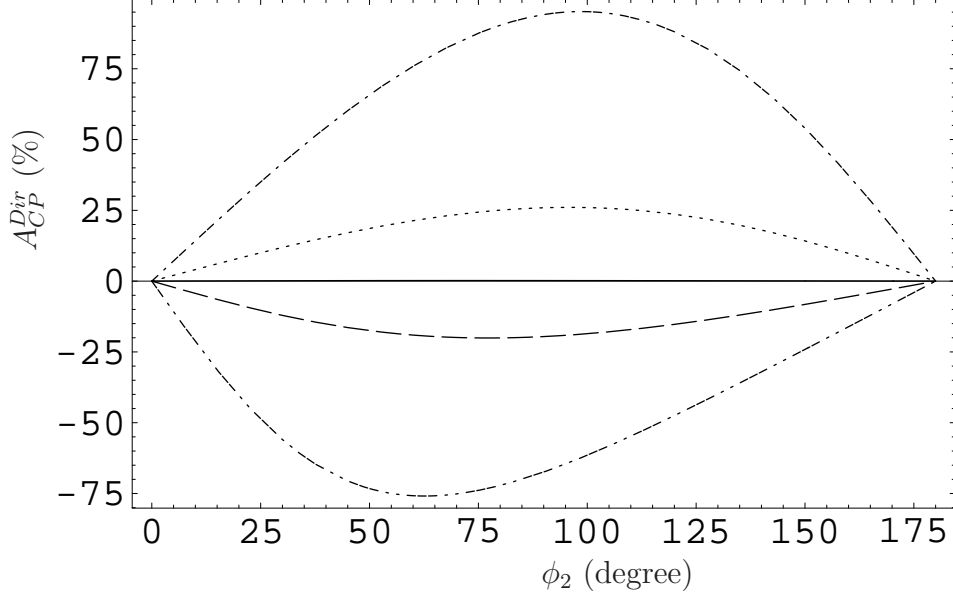


Figure 7: Direct CP violation parameters of $B^+ \rightarrow \pi^+ \omega$ (solid line), $B^+ \rightarrow \pi^+ \rho^0$ (dotted line), $B^+ \rightarrow \rho^+ \pi^0$ (dashed line), $B^0 \rightarrow \rho^0 \pi^0$ (dash-dotted line), $B^0 \rightarrow \pi^0 \omega$ (dash-dotted-dotted line), as a function of CKM angle ϕ_2 .

violation parameter is defined as

$$a_{\epsilon+\epsilon'} = \frac{-2\text{Im}(\lambda_{CP})}{1 + |\lambda_{CP}|^2}, \quad (61)$$

where

$$\lambda_{CP} = \frac{V_{tb}^* V_{td} \langle f | H_{eff} | \bar{B}^0 \rangle}{V_{tb} V_{td}^* \langle f | H_{eff} | B^0 \rangle}. \quad (62)$$

Using equations (49,50), we can derive as

$$\lambda_{CP} = e^{2i\phi_2} \frac{1 + ze^{i(\delta-\phi_2)}}{1 + ze^{i(\delta+\phi_2)}}. \quad (63)$$

λ_{CP} and $a_{\epsilon+\epsilon'}$ are functions of CKM angle ϕ_2 only. Therefore, the CP asymmetry of $B \rightarrow \pi\rho$ and $\pi\omega$ decays can measure the CKM angle ϕ_2 , even if for the neutral B decays including the $B\bar{B}$ mixing effect.

If we integrate the time variable t , we will get the total CP asymmetry as

$$A_{CP} = \frac{1}{1+x^2} A_{CP}^{dir} + \frac{x}{1+x^2} a_{\epsilon+\epsilon'}, \quad (64)$$

with $x = \Delta m/\Gamma \simeq 0.723$ for the $B^0 - \bar{B}^0$ mixing in SM [19]. The total CP asymmetries of $B^0 \rightarrow \pi^0 \rho^0$, $\pi^0 \omega$ are shown in Figure 8. Although the CP asymmetries are large, but it is still difficult to measure for experiments, since their branching ratios are small around 10^{-7} .

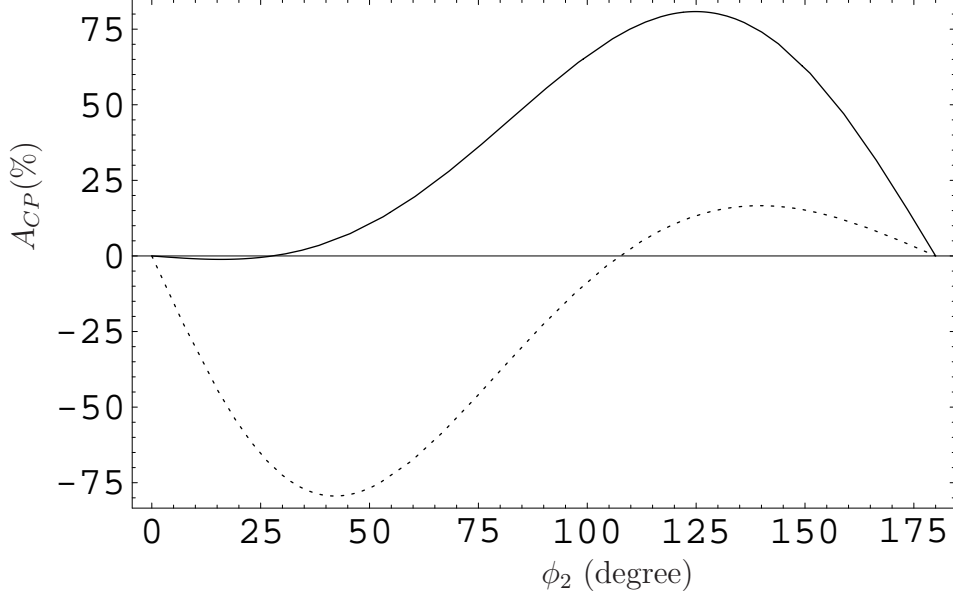


Figure 8: Total CP asymmetries of $B^0 \rightarrow \pi^0 \rho^0$ (solid line), and $B^0 \rightarrow \pi^0 \omega$ (dotted line), as a function of CKM angle ϕ_2 .

The CP asymmetries of $B^0/\bar{B}^0 \rightarrow \pi^\pm \rho^\mp$ are very complicated. Here one studies the four time-dependent decay widths for $B^0(t) \rightarrow \pi^+ \rho^-$, $\bar{B}^0(t) \rightarrow \pi^- \rho^+$, $B^0(t) \rightarrow \pi^- \rho^+$ and $\bar{B}^0(t) \rightarrow \pi^+ \rho^-$ [26, 27, 28]. These time-dependent widths can be expressed by four basic matrix elements

$$\begin{aligned} g &= \langle \pi^+ \rho^- | H_{eff} | B^0 \rangle, & h &= \langle \pi^+ \rho^- | H_{eff} | \bar{B}^0 \rangle, \\ \bar{g} &= \langle \pi^- \rho^+ | H_{eff} | \bar{B}^0 \rangle, & \bar{h} &= \langle \pi^- \rho^+ | H_{eff} | B^0 \rangle, \end{aligned} \quad (65)$$

which determine the decay matrix elements of $B^0 \rightarrow \pi^+ \rho^-$ & $\pi^- \rho^+$ and of $\bar{B}^0 \rightarrow \pi^- \rho^+$ & $\pi^+ \rho^-$ at $t = 0$. The matrix elements g and \bar{h} are given in eq.(30,31). The matrix elements h and \bar{g} are obtained from \bar{h} and g by changing the signs of the weak phases contained in the products of the CKM matrix elements. We also need to know the CP-violating parameter coming from the $B^0 - \bar{B}^0$ mixing. Defining:

$$\begin{aligned} B_1 &= p|B^0\rangle + q|\bar{B}^0\rangle, \\ B_2 &= p|B^0\rangle - q|\bar{B}^0\rangle, \end{aligned} \quad (66)$$

with $|p|^2 + |q|^2 = 1$ and $q/p = \sqrt{H_{21}/H_{12}}$, with $H_{ij} = M_{ij} - i/2\Gamma_{ij}$ representing the $|\Delta B| = 2$ and $\Delta Q = 0$ Hamiltonian. For the decays of B^0 and \bar{B}^0 , we use,

$$\frac{q}{p} = \frac{V_{tb}^* V_{td}}{V_{tb} V_{td}^*} = e^{-2i\phi_1}. \quad (67)$$

So, $|q/p| = 1$, and this ratio has only a phase given by $-2\phi_1$. Then, the four time-dependent widths are given by the following formulae (we follow the notation of [28]):

$$\begin{aligned}
\Gamma(B^0(t) \rightarrow \pi^+ \rho^-) &= e^{-\Gamma t} \frac{1}{2} (|g|^2 + |h|^2) \{1 + a_{\epsilon'} \cos \Delta m t + a_{\epsilon+\epsilon'} \sin \Delta m t\}, \\
\Gamma(\bar{B}^0(t) \rightarrow \pi^- \rho^+) &= e^{-\Gamma t} \frac{1}{2} (|\bar{g}|^2 + |\bar{h}|^2) \{1 - a_{\bar{\epsilon}'} \cos \Delta m t - a_{\epsilon+\bar{\epsilon}'} \sin \Delta m t\}, \\
\Gamma(B^0(t) \rightarrow \pi^- \rho^+) &= e^{-\Gamma t} \frac{1}{2} (|\bar{g}|^2 + |\bar{h}|^2) \{1 + a_{\bar{\epsilon}'} \cos \Delta m t + a_{\epsilon+\bar{\epsilon}'} \sin \Delta m t\}, \\
\Gamma(\bar{B}^0(t) \rightarrow \pi^+ \rho^-) &= e^{-\Gamma t} \frac{1}{2} (|g|^2 + |h|^2) \{1 - a_{\epsilon'} \cos \Delta m t - a_{\epsilon+\epsilon'} \sin \Delta m t\}, \tag{68}
\end{aligned}$$

where

$$\begin{aligned}
a_{\epsilon'} &= \frac{|g|^2 - |h|^2}{|g|^2 + |h|^2}, & a_{\epsilon+\epsilon'} &= \frac{-2Im\left(\frac{q}{p} \frac{h}{g}\right)}{1 + |h/g|^2}, \\
a_{\bar{\epsilon}'} &= \frac{|\bar{h}|^2 - |\bar{g}|^2}{|\bar{h}|^2 + |\bar{g}|^2}, & a_{\epsilon+\bar{\epsilon}'} &= \frac{-2Im\left(\frac{q}{p} \frac{\bar{g}}{\bar{h}}\right)}{1 + |\bar{g}/\bar{h}|^2}. \tag{69}
\end{aligned}$$

We calculate the above four CP violation parameters related to $B^0/\bar{B}^0 \rightarrow \pi^\pm \rho^\mp$ decays in PQCD. The results are shown in Fig.9 as a function of ϕ_2 . Comparing the results with the factorization approach [24], we found that our predicted size of $a_{\epsilon'}$ and $a_{\bar{\epsilon}'}$ are smaller while $a_{\epsilon+\epsilon'}$ and $a_{\epsilon+\bar{\epsilon}'}$ are larger. By measuring the time-dependent spectrum of the decay rates of B^0 and \bar{B}^0 , one can find the coefficients of the two functions $\cos \Delta m t$ and $\sin \Delta m t$ in eq.(68) and extract the quantities $a_{\epsilon'}$, $a_{\epsilon+\epsilon'}$, $a_{\bar{\epsilon}'}$, and $a_{\epsilon+\bar{\epsilon}'}$. Using these experimental results, we can tell the size of CKM angle ϕ_2 from Fig.9.

5 Summary

We calculate the $B^0 \rightarrow \pi^+ \rho^-$, $B^0 \rightarrow \rho^+ \pi^-$, $B^+ \rightarrow \rho^+ \pi^0$, $B^+ \rightarrow \pi^+ \rho^0$, $B^0 \rightarrow \pi^0 \rho^0$, $B^+ \rightarrow \pi^+ \omega$ and $B^0 \rightarrow \pi^0 \omega$ decays, together with their charge conjugate modes, in a perturbative QCD approach. We calculate the $B \rightarrow \pi$ and $B \rightarrow \rho$ form factors, which are in agreement with the QCD sum rule calculations. In addition to the usual factorization contributions, we also calculate the non-factorizable and annihilation diagrams. Although they are sub-leading contributions in the branching ratios of these decays, they are not negligible. Furthermore these diagrams provide the necessary strong phases required by the direct CP asymmetry measurement.

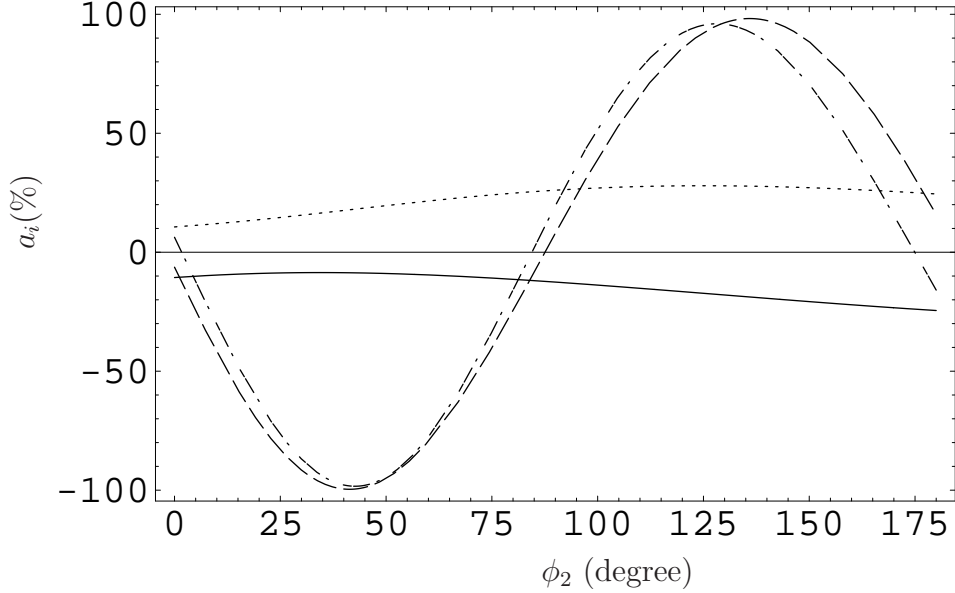


Figure 9: CP violation parameters of $B^0/\bar{B}^0 \rightarrow \pi^\pm \rho^\mp$ decays: $a_{\epsilon'}$ (solid line), $a_{\bar{\epsilon}'}$ (dotted line), $a_{\epsilon+\epsilon'}$ (dashed line) and $a_{\epsilon+\bar{\epsilon}'}$ (dash-dotted line) as a function of CKM angle ϕ_2 .

Our calculation gives the right branching ratios, which agrees well with the CLEO and BABAR measurements. We also predict large direct CP asymmetries in $B^+ \rightarrow \rho^+ \pi^0$ and $B^+ \rightarrow \pi^+ \rho^0$ decays. Including the $B\bar{B}$ mixing effect, the CP asymmetries of $B^0 \rightarrow \pi^0 \omega$ and $B^0 \rightarrow \pi^0 \rho^0$ are very large, but their branching ratios are small in SM. The CP asymmetry parameters of $B^0 \rightarrow \pi^+ \rho^-$, $B^0 \rightarrow \rho^+ \pi^-$ decays require the time dependent measurement of branching ratios.

Acknowledgments

We thank our PQCD group members: Y.Y. Keum, E. Kou, T. Kurimoto, H.N. Li, T. Morozumi, A.I. Sanda, N. Sinha, R. Sinha, K. Ukai and T. Yoshikawa for helpful discussions. This work was supported by the Grant-in-Aid for Scientific Research on Priority Areas (Physics of CP violation). We also thank JSPS for support.

A Related functions defined in the text

We show here the function h_i 's, coming from the Fourier transform of $H^{(0)}$,

$$\begin{aligned} h_e(x_1, x_2, b_1, b_2) = & K_0(\sqrt{x_1 x_2} m_B b_1) [\theta(b_1 - b_2) K_0(\sqrt{x_2} m_B b_1) I_0(\sqrt{x_2} m_B b_2) \\ & + \theta(b_2 - b_1) K_0(\sqrt{x_2} m_B b_2) I_0(\sqrt{x_2} m_B b_1)] S_t(x_2) \end{aligned} \quad (70)$$

$$\begin{aligned} h_d(x_1, x_2, x_3, b_1, b_2) = & \alpha_s(t_d) K_0(-i\sqrt{x_2 x_3} m_B b_2) \\ & \times [\theta(b_1 - b_2) K_0(\sqrt{x_1 x_2} m_B b_1) I_0(\sqrt{x_1 x_2} m_B b_2) \\ & + \theta(b_2 - b_1) K_0(\sqrt{x_1 x_2} m_B b_2) I_0(\sqrt{x_1 x_2} m_B b_1)] \end{aligned} \quad (71)$$

$$\begin{aligned} h_f^1(x_1, x_2, x_3, b_1, b_2) = & K_0(-i\sqrt{x_2 x_3} m_B b_1) \alpha_s(t_f^1) \\ & \times [\theta(b_1 - b_2) K_0(-i\sqrt{x_2 x_3} m_B b_1) J_0(\sqrt{x_2 x_3} m_B b_2) \\ & + \theta(b_2 - b_1) K_0(-i\sqrt{x_2 x_3} m_B b_2) J_0(\sqrt{x_2 x_3} m_B b_1)] \end{aligned} \quad (72)$$

$$\begin{aligned} h_f^2(x_1, x_2, x_3, b_1, b_2) = & K_0(\sqrt{x_2 + x_3 - x_2 x_3} m_B b_1) \alpha_s(t_f^2) \\ & \times [\theta(b_1 - b_2) K_0(-i\sqrt{x_2 x_3} m_B b_1) J_0(\sqrt{x_2 x_3} m_B b_2) \\ & + \theta(b_2 - b_1) K_0(-i\sqrt{x_2 x_3} m_B b_2) J_0(\sqrt{x_2 x_3} m_B b_1)] \end{aligned} \quad (73)$$

$$\begin{aligned} h_a(x_1, x_2, b_1, b_2) = & K_0(-i\sqrt{x_1 x_2} m_B b_2) S_t(x_1) \\ & \times [\theta(b_1 - b_2) K_0(-i\sqrt{x_1} m_B b_1) J_0(\sqrt{x_1} m_B b_2) \\ & + \theta(b_2 - b_1) K_0(-i\sqrt{x_1} m_B b_2) J_0(\sqrt{x_1} m_B b_1)], \end{aligned} \quad (74)$$

where J_0 is the Bessel function and K_0, I_0 are modified Bessel functions $K_0(-ix) = -(\pi/2)Y_0(x) + i(\pi/2)J_0(x)$. The threshold resummation form factor $S_t(x_i)$ is adopted from ref.[13]

$$S_t(x) = \frac{2^{1+2c}\Gamma(3/2+c)}{\sqrt{\pi}\Gamma(1+c)} [x(1-x)]^c, \quad (75)$$

where the parameter $c = 0.3$. This function is normalized to unity.

The Sudakov factors used in the text are defined as

$$\begin{aligned} S_{ab}(t) = & s(x_1 m_B / \sqrt{2}, b_1) + s(x_2 m_B / \sqrt{2}, b_2) + s((1-x_2) m_B / \sqrt{2}, b_2) \\ & - \frac{1}{\beta_1} \left[\ln \frac{\ln(t/\Lambda)}{-\ln(b_1 \Lambda)} + \ln \frac{\ln(t/\Lambda)}{-\ln(b_2 \Lambda)} \right], \\ S_{cd}(t) = & s(x_1 m_B / \sqrt{2}, b_1) + s(x_2 m_B / \sqrt{2}, b_2) + s((1-x_2) m_B / \sqrt{2}, b_2) \\ & + s(x_3 m_B / \sqrt{2}, b_1) + s((1-x_3) m_B / \sqrt{2}, b_1) \end{aligned} \quad (76)$$

$$-\frac{1}{\beta_1} \left[2 \ln \frac{\ln(t/\Lambda)}{-\ln(b_1\Lambda)} + \ln \frac{\ln(t/\Lambda)}{-\ln(b_2\Lambda)} \right], \quad (77)$$

$$\begin{aligned} S_{ef}(t) = & s(x_1 m_B / \sqrt{2}, b_1) + s(x_2 m_B / \sqrt{2}, b_2) + s((1-x_2) m_B / \sqrt{2}, b_2) \\ & + s(x_3 m_B / \sqrt{2}, b_2) + s((1-x_3) m_B / \sqrt{2}, b_2) \\ & - \frac{1}{\beta_1} \left[\ln \frac{\ln(t/\Lambda)}{-\ln(b_1\Lambda)} + 2 \ln \frac{\ln(t/\Lambda)}{-\ln(b_2\Lambda)} \right], \end{aligned} \quad (78)$$

$$\begin{aligned} S_{gh}(t) = & s(x_2 m_B / \sqrt{2}, b_1) + s(x_3 m_B / \sqrt{2}, b_2) + s((1-x_2) m_B / \sqrt{2}, b_1) \\ & + s((1-x_3) m_B / \sqrt{2}, b_2) - \frac{1}{\beta_1} \left[\ln \frac{\ln(t/\Lambda)}{-\ln(b_1\Lambda)} + \ln \frac{\ln(t/\Lambda)}{-\ln(b_2\Lambda)} \right], \end{aligned} \quad (79)$$

where the function $s(q, b)$ are defined in the Appendix A of ref.[10]. The scale t_i 's in the above equations are chosen as

$$t_e^1 = \max(\sqrt{x_2} m_B, 1/b_1, 1/b_2), \quad (80)$$

$$t_e^2 = \max(\sqrt{x_1} m_B, 1/b_1, 1/b_2), \quad (81)$$

$$t_d = \max(\sqrt{x_1 x_2} m_B, \sqrt{x_2 x_3} m_B, 1/b_1, 1/b_2), \quad (82)$$

$$t_f^1 = \max(\sqrt{x_2 x_3} m_B, 1/b_1, 1/b_2), \quad (83)$$

$$t_f^2 = \max(\sqrt{x_2 x_3} m_B, \sqrt{x_2 + x_3 - x_2 x_3} m_B, 1/b_1, 1/b_2). \quad (84)$$

References

- [1] A. Gritsan, et al., CLEO Collaboration, talk at Lake Louis Winter Institute, Feb. 20-26, 2000.
- [2] H.R. Quinn and J.P. Silva, preprint hep-ph/0001290; A. Deandrea et al., preprint hep-ph/0002038; M.Z. Yang, Y.D. Yang, Phys. Rev. D62, 114019 (2000).
- [3] D.S. Du, Z.Z. Xing, Phys. Rev. D48, 4155 (1993); G. Kramer, W.F. Palmer, H. Simma, Z. Phys. C66, 429 (1995); A. Ali, G. Kramer and C.D. Lü, Phys. Rev. D58, 094009 (1998); C.D. Lü, Nucl. Phys. Proc. Suppl. 74, 227 (1999).
- [4] Y.-H. Chen, H.-Y. Cheng, B. Tseng, K.-C. Yang, Phys. Rev. D60, 094014 (1999).
- [5] C.H. Chang, H.N. Li, Phys. Rev. D55, 5577 (1997); T.W. Yeh and H.N. Li, Phys. Rev. D56, 1615 (1997).

- [6] H.N. Li, H.L. Yu, Phys. Rev. Lett. 74, 4388 (1995); Phys. Lett. B353, 301 (1995); Phys. Rev. D53, 2486 (1996).
- [7] H.N. Li, Phys. Rev. D52, 3958 (1995).
- [8] H.N. Li, hep-ph/0102013.
- [9] For a review, see G. Buchalla, A.J. Buras, M.E. Lautenbacher, Rev. Mod. Phys. 68, 1125 (1996).
- [10] C.D. Lü, K. Ukai, M.Z. Yang, Phys. Rev. D63, 074009 (2001).
- [11] A.G. Grozin, M. Neubert, Phys. Rev. D55, 272 (1997); M. Beneke, T. Feldmann, Nucl. Phys. B592, 3 (2001).
- [12] M. Beneke, G. Buchalla, M. Neubert, C.T. Sachrajda, Nucl. Phys. B591, 313 (2000).
- [13] T. Kurimoto, H.-n. Li, A.I. Sanda, hep-ph/0105003.
- [14] Y.Y. Keum, H.-n. Li, A.I. Sanda, Phys. Lett. B504, 6 (2001); Phys. Rev. D63, 054008 (2001); C.-h. Chen and H.-n. Li, Phys. Rev. D63, 014003 (2000).
- [15] For example, see: M. Beneke, G. Buchalla, M. Neubert, C.T. Sachrajda, Phys. Rev. Lett. 83, 1914 (1999); Dong-sheng Du, De-shan Yang, Guo-huai Zhu, Phys. Rev. D64, 014036 (2001); Hai-Yang Cheng, Kwei-Chou Yang, Phys. Rev. D63, 074011 (2001); Mao-Zhi Yang, Ya-Dong Yang, Phys. Rev. D62, 114019 (2000).
- [16] V.M. Braun and I.E. Filyanov, Z Phys. C48, 239 (1990); P. Ball, J. High Energy Phys. 01,010 (1999).
- [17] P. Ball, V.M. Braun, Y. Koike, and K. Tanaka, Nucl. Phys. B529, 323 (1998).
- [18] P. Ball and V.M. Braun, Phys. Rev. D58, 094016 (1998); P. Ball, J. High Energy Phys. 9809, 005 (1998).
- [19] Particle Data Group, Eur. Phys. J. C15, 1 (2000).
- [20] B. Aubert et al., BABAR Collaboration, hep-ex/0107058.

- [21] B.Aubert et al., BABAR Collaboration, hep-ex/0108017.
- [22] P. Chang, talk given at International Europhysics Conference On High-Energy Physics, 12-18 July, 2001, Budapest, Hungary; and private communications.
- [23] M. Bander, D. Silverman, and A. Soni, Phys. Rev. Lett. 43, 242 (1979).
- [24] A. Ali, G. Kramer and C.D. Lü, Phys. Rev. D59, 014005 (1999).
- [25] S. Chen, et al., CELO Collaboration, hep-ex/0001009.
- [26] M. Gronau, Phys. Lett. **B233**, 479 (1989).
- [27] R. Aleksan, I. Dunietz, B. Kayser and F. Le Diberder, Nucl. Phys. **B361**, 141 (1991).
- [28] W.F. Palmer and Y.L. Wu, Phys. Lett. **B350**, 245 (1995).